Spin Texture Engineering by a Temperature Gradient in Ultrathin CoFeB Film

Xiangyu Zheng[1,2‡], Kangning Xu[1‡], Wenjia Li[3‡], Chen Xiao[1], Guanqi Li[4], Kaiyu Tong[3], Hao Tan [1], Junlin Wang[4*], Jing Wu[4,3*], Yongbing Xu[3*]

[1)] Fert Beijing Institute, MIIT Key Laboratory of Spintronics, School of Integrated Circuit Science and Engineering, Beihang University, Beijing, 100191, China

[2)]National Key Laboratory of Spintronics, Hangzhou International Innovation Institute, Beihang University, Hangzhou 311115, China

[3)]School of Physics, Engineering and Technology, University of York, York, YO10 5DD, UK

[4)]School of Integrated Circuits, Guangdong University of Technology, Guangzhou 510006, China

Abstract— Magnetic texture in a chiral material is touted as one of the next-generation non-volatile computing elements. Thermal manipulation of magnetic textures attracts considerable attention and has promising applications. Here, the temperature-dependent magnetic properties of Ta/CoFeB/MgO thin film are studied experimentally and theoretically. We report the controllable spin texture distribution with a temperature gradient in the Ta/CoFeB/MgO thin film. The nucleation area could be generated at certain location through the cooperation of heat and magnetic field. This method offers a way to realize spin texture injection at specific positions in magnetic thin films and devices. This work provides useful guidelines for the thermal control of the spintronic device operation.

Keywords: Spin texture, Chiral material, Atomistic spin simulation, Temperature gradient

‡ Contributions: Xiangyu Zheng, Kangning Xu and Wenjia Li contributed equally to this work.

*Author to whom correspondence should be addressed: junlin.wang@gdut.edu.cn; jing.wu@york.ac.uk, yongbing.xu@york.ac.uk

1. Introduction

Chiral spin texture in the ferromagnetic material in contact to a heavy non-magnetic metal can be tweaked with a magnetic field. The chiral interaction between the atoms in the heavy mental and ferromagnetic system is known as the Dzyaloshinskii–Moriya interaction (DMI)[1-3]. The DMI at the interface between the strong spin orbit coupling (SOC) layer and the ferromagnetic layer enhances the stability of the chiral spin textures such as the magnetic skyrmion[4-6] and hemochorial Neel-type domain walls (DWs)[7]. The manipulation of chiral spin structures using magnetic anisotropy gradients holds significant research value for future low-power storage and in-memory computing device technologies[8-10]. The gradient of magnetic anisotropy can be created by producing a thickness gradient in the magnetic layer, leading to gradient changes in the magnetic domain phase within the film.[11, 12]. Wedge-shaped nanostructure, for example, can yield magnetic anisotropy gradient[13]. A strain-accessed sample will also have a magnetic anisotropy distribution[12, 14]. In addition to the research on the control of perpendicular magnetic anisotropy (PMA) gradients by structure, temperature as an important parameter also has an impact on the anisotropy energy of the system. The temperature difference can significantly affect the magnetic properties and even the performance of the whole device. Many interesting phenomena arises from the ferromagnetic system, such as Skyrmion generation and domain wall manipulation, when thermal gradient induced[15-19]. Therefore, the study of thermal effect on magnetic material is essential and the use of thermal effect can open a new branch in spintronic applications.

However, the specific changes on magnetic properties caused by thermal gradient remains an open question. In this work, we study the influence of the different temperatures and temperature gradients on the magnetization reversal of perpendicular magnetic anisotropy CoFeB-based thin film. We have found that the thermal gradient can be used to control the spin texture nucleation area and realize the controllable spin texture creation in ferromagnetic material.

2. Experiment

All the samples in this study were deposited on thermally oxidized Si wafers (100) by magnetron sputtering at RT with base pressure better than 5×10^{-5} *Torr*. The samples consist of, from the substrate side, Ta(5)/MgO(3)/CoFeB(t)/Ta(5)(number are nominal thickness in nanometers). The thickness of the CoFeB (1.0-1.4 *nm*) layer is varied across the films studied in this work. The PMA of these sample originates from the Fe-O hybridization and B away from interface, and annealing can assist the interface recrystallization which can enhance the PMA of CoFeB thin film system. Therefore, the deposited films were annealed in a high vacuum furnace chamber at 300 ºC for 30 min.

3. Experimental measurement

The in-plane and out-of-plane magnetization versus external magnetic field (M-H) curves for Substrate/Ta(5)/MgO(3)/CoFeB(t)/Ta(5) are measured by a vibrating sample magnetometer (VSM). According to the magnetization curves of these samples, Ta(5)/MgO(3)/CoFeB(1.4)/Ta(5) exhibits strong PMA which discussed in this work. To study the thermal effect on magnetism, the sample is measured in the temperature range of 150*K* to 500*K* with 50*K* steps. A series of typical out of plane magnetization curves are shown in Fig. 1a. The magnetization curves show that the overall magnetic properties of the sample vary with temperature. The Coercivity increases at low temperatures and decreases at high temperatures. Another significant change is that the saturation magnetic moment (M) decreases with increasing temperature. Figure 1b shows the in-plane and out of plane hysteresis loops measured using VSM at a temperature of 500*K*. The result of measurements indicate that the PMA is significantly weakened at high temperatures and there is a trend of crossover from out-of-plane to in-plane. Fig.1c shows the dependence of saturation magnetization intensity M_s on temperature, which is determined by dividing the spontaneous magnetic moment per unit area M by the effective CoFeB thickness t (1.4 *nm*), ranging from 150*K* to 500*K*. Within the experimental errors, the M_s in CoFeB thin films showed a monotonic decreasing trend. The rate of change of M_s at high temperatures is significantly higher than that at low temperatures, indicating that the PMA of CoFeB is more susceptible to influence at high temperatures.

The effective perpendicular anisotropy energy density K_{eff} is positively correlated with the M_s and effective perpendicular anisotropy field H_k. Due to the monotonic decrease of M_s and H_k with temperature, K_{eff} also exhibits a temperature dependent decrease. The interfacial anisotropy plays a domain role for perpendicular anisotropy in MgO/CoFeB system[20, 21], therefore, the interfacial anisotropy energy density K_i also decreases with increasing temperature.

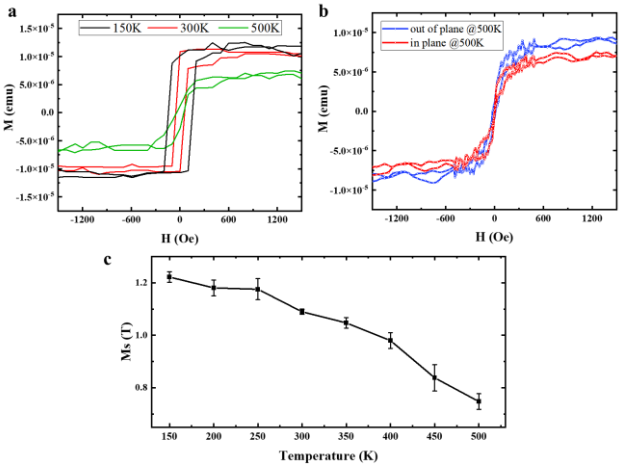

Fig. 1 Temperature dependence magnetic properties of CoFeB thin film. (a) the out-of-plane magnetization curves measured by vibrating sample magnetometer (VSM) at different temperature. (b) in-plane and out-of-plane magnetization curves for MgO/CoFeB measured by the VSM at 500*K*. (c) temperature dependence of spontaneous magnetization M_s for MgO/CoFeB from 150*K* to 500*K*.

The temperature variable magneto-optical Kerr effect (MOKE) experiment is achieved by using the MicrostatHe-R cryostat, as shown in Fig. 2a. The MicrostatHe-R can provide a wide temperature range from 2.2*K* to 500*K*[22]. The magnetization curves measured by MOKE are obtained after the temperature reaches a preset value and stabilizes. In this temperature change experiment, the temperature range is 200*K* to 340*K*. Fig. 2b shows the temperature-dependent hysteresis loops of CoFeB thin film measured by MOKE. The out-of-plane magnetization curves with magnetization (M) is normalized to the saturation magnetization (M_s). The variation trend of coercivity measured by MOKE is consistent with the results of VSM, that is, it increases with decreasing temperature. The black semi-square loop measured at a temperature of 220*K* indicates that the sample requires a larger external magnetic field to reverse magnetization. However, a smaller applied magnetic field can reverse the magnetization of CoFeB at 310*K*, which is shown as the violet curved loop. The MOKE images of spin texture evolved for Ta(5)/MgO(3)/CoFeB(1.4)/Ta(5) (in nm) thin film via various temperature is showing in Fig. 2c to f. Those MOKE images which picked up at zero Kerr signal point (position of coercivity), demonstrate that the domain size changes significantly during the temperature change process. Fig. 2g shows the trend of changes in domain size with error bar. We first generate a grayscale distribution map of the MOKE images, select 10 magnetic domains on the map, and estimate the average width of the magnetic domains by analyzing the intermediate number of gray value jump. We repeat the experiment on the same sample for five times, draw the average width of the magnetic domain according to the above method. The domain size displays monotonic decrease with increasing temperature, and the largest domain size at 200*K* is around twice as wide as the smallest domain size at 340*K*.

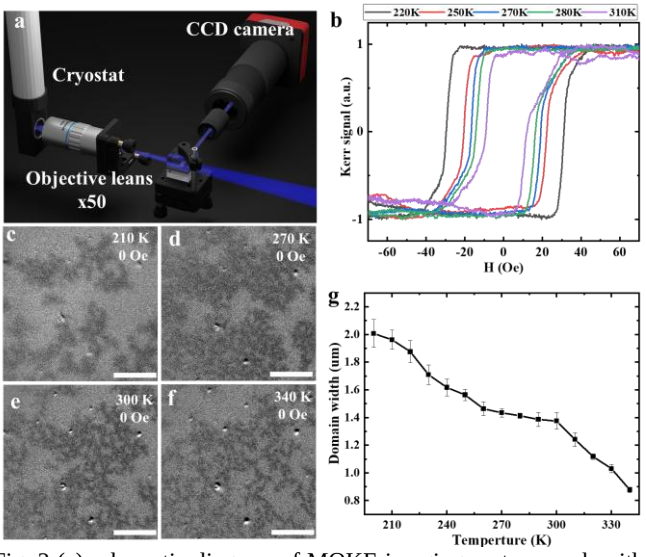

Fig. 2 (a) schematic diagram of MOKE imaging system work with cryostat. (b) out-of-plane temperature-dependent hysteresis loops with magnetization (M) normalized to the saturation magnetization (M_s). Polar-MOKE images illustrate the domain size evolved via temperature vary from 210 to 340 *K* as shown in c to f. The scale bar is 10 μm. (g) Domain size evolved versus temperature various.

The size of the chiral magnetic domain is not only related to magnetic anisotropy K, but also the exchange stiffness A and Dzyaloshinskii-Moriya interaction (DMI) D[23]. Due to the magnitude of the K is much larger than that of the A and D, the domain size is determined by the magnetic anisotropic. Although K, A and D can vary with the temperature, the change of domain size is dominated by K. According to the temperature dependent characteristic of CoFeB, the magnetic anisotropy gradient can be realized by inducing a temperature gradient. Here, we demonstrate a method of magnetic anisotropy gradient created by temperature gradient induced and observed by MOKE microscopy. We designed a sample stage based on the characteristics of temperature difference produced by Peltier module as shown in Fig. 3a. The temperature gradient generator is machined from three pieces of aluminum and sandwiched a Peltier module. The part at the front contacts the cold side of the Peltier module and cools the lower half of the sample. The middle part touches the hot side of the Peltier module, which will heat the top half of the sample

while dissipating excess heat to the environment. The rear part is used to hold the entire device and allow air to flow over the radiator. Under different working voltages, the Peltier module can provide temperature differences to yield a temperature gradient. The temperature distribution is captured by an infrared camera as shown in Fig. 3b. We use thermal conductive tape to stick on the sample to measure the temperature accurately, which avoids temperature measurement error caused by metal reflection.

To verify the temperature gradient generator could achieve thermal balance at a certain temperature, we performed thermal steady state and thermal transient simulations on the device. The simulated environment was set to isothermal boundaries with an ambient temperature of 20℃ and the device was immersed in air. The air around the radiator is set to move at a speed of $0.1 m/s$ from bottom to top that limited by the simulation scale. The thermal resistance of the contact surface between the sample and the device is $0.13 K/W$ according to the specifications of thermal grease. In the laboratory, the airflow speed at the heat sink can be much higher than in the simulated environment, to compensate for lower wind speed issues in the simulation, the current heating of the Peltier module is reduced to $2W$ (~$10W$ in the real-world). Thus, the simulation conditions of the heat source are -$5W$ on the cold side and $7W$ on the hot side. Simulation results show that the design generated a temperature gradient of 35.4 to 46.2℃ on the surface of the silicon sample when it reaches thermal stability (as shown in Fig. 3c).

The thin films of Ta(5)/MgO(3)/CoFeB(1.4)/Ta(5) with perpendicular magnetic anisotropy is measured by MOKE imagining system via temperature gradient generator sample stage. We first take the MOKE images of domain evolution at room temperature as the reference which is illustrated in Fig. 3c to e. The nucleation randomly appears at first stage and subsequently the magnetic domains extend evenly from nucleation. Finally the magnetization of the system is reversed. The working voltage of chilling plate is selected at $1.5V$, which yields a range of temperature distribution at the gap for 30℃ to 43℃ ($303K$-$316K$). The gap between the upper and lower edges is 0.5mm, and the calculated temperature gradient in the sample is $\Delta T = 0.026 K\mu m^{-1}$. The domain is first generated at the hot side and then expanded while few nucleation points or domain structure existed at the cold side as shown in Fig. 3g to i. Eventually, the domain structure is extended to the whole view and will reverse till saturation.

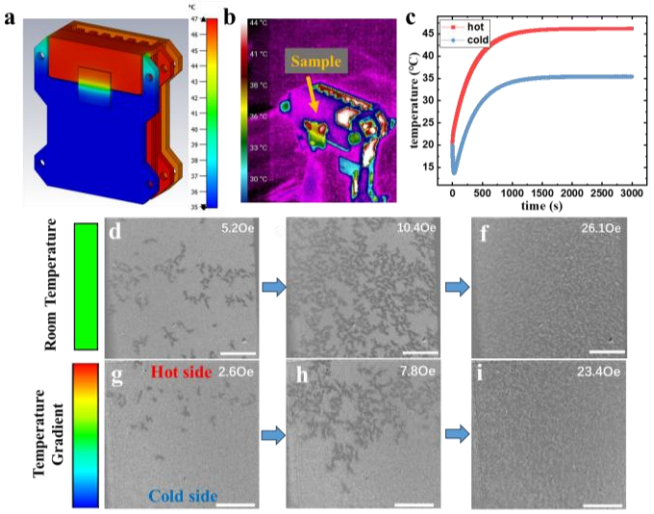

Fig. 3 (a) The simulation result of stage with silicon substrate. The colorful distribution on the silicon substrate corresponds to the temperature gradient. (b) The temperature distribution is captured by an infrared camera. The color mapping corresponds to the magnitude of temperature. The white rectangular sketches the sample position. (c) the simulation results of temperature gradient generator that can realize stable thermal balance. Polar-MOKE images illustrate the domain structure evolved under external magnetic field at room temperature (d to f) and under temperature gradient (g to i), respectively. The scale bar is 20 μm.

From the results in Fig. 3d to f, when the external magnetic field increase, the maze domain will nucleate in the whole thin film area. In Fig. 3g to i, the domain first nucleates at the area with a higher temperature which is different from the results in Fig. 3d to f. According to the hysteresis, the temperature gradient gives a distribution of the varying coercivity to the thin film system. For the area with higher temperature, the maze domain nucleation requires a lower external field, which means the temperature gradient can help the system modulate the area of magnetic domain nucleation.

4. Atomistic spin model

The domain energy under different temperature is studied by the atomistic spin dynamics model. The atomistic simulation in this work is provided by the Vampire 5 software package[24, 25]. The energy of the system is described by the following Hamiltonian, which includes all the energy contribution to the magnetic behavior of the system, including the Heisenberg form of exchange:

$$\mathrm{H} = -\sum_{i<j} J_{ij}\vec{S_i}\cdot\vec{S_j} - \sum_i k_u^i\left(\vec{S_i}\cdot\hat{e}\right) - \mu_0\sum_i \mu_S^i\vec{S_i}\cdot\overrightarrow{H_{app}} + H_{demag}, \quad (1)$$

Where the Jij is the exchange interaction between the spins on site i and j, k_u^i is the uniaxial anisotropy energy on site i along the axis ê, and μ_S^i is the atomic

spin moment on the atomic site i in unit of μ_B and μ_0 is the permeability constant. The parameters in this equation can be measured experimentally or calculated by ab-initio density functional theory (DFT) calculations. In this model, the perpendicular magnetic anisotropy of the CoFeB thin film is provided by the interface between the CoFeB and MgO interface. The parameters for the atomistic simulation is obtained from the Ref.[25-26].

Table 1. Adopted model parameters in the atomistic simulation

	CoFeB(interface) with MgO)	CoFeB(bulk)	Unit
J_{ij}	1.547×10^{-20}	7.735×10^{-21}	J link^{-1}
μ_S	1.60	1.60	μ_B
k_u	1.35×10^{-22}	0.0	J atom^{-1}

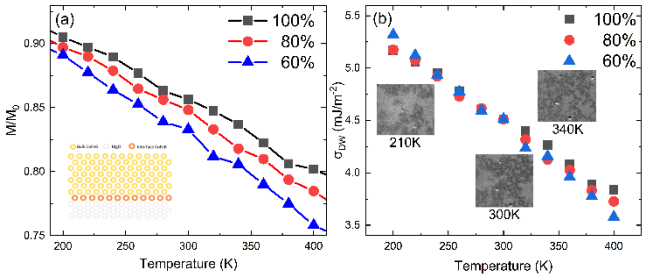

Fig. 4 (a) Temperature dependent mean magnetization of the thin film with different density of interface CoFeB atoms calculated by the atomistic spin dynamics model. (b) Temperature dependent of the domain energy with different density of interface CoFeB atoms.

From the simulation results in Fig. 4, the CoFeB/MgO interface of the system is considered as different densities of interface CoFeB atoms because the unoxidized Mg atoms will affect the interface perpendicular anisotropy. The temperature dependent magnetization is given in Fig. 4a, where the magnetization under thermal effect is influenced by the density of the interface CoFeB atoms. The interface CoFeB atoms have higher exchange stiffness and magnetic anisotropy than the bulk CoFeB atoms and will be more stable under thermal effect. The temperature dependent magnetic anisotropy K(T), exchange stiffness A(T) and Dzyaloshinskii–Moriya interaction(DMI) D(T) are calculated from the temperature dependent magnetization M(T)[26]. The K(300), A(300) and D(300) are the magnetic parameters measured from the experiment and can be used to calculate the parameters without thermal effect (K(0), A(0), D(0)) following the equations which are given below:

$$\begin{aligned} K(T) &= K(0)M(T)^{\gamma} \\ A(T) &= A(0)M(T)^{\beta} \\ D(T) &= D(0)M(T)^{\beta} \end{aligned} \quad (2)$$

The γ and β are constants where are set as 3.03 and 1.5, respectively[26]. The constant shows that when the temperature increase the effect magnetic anisotropy will drop faster than the exchange energy and DMI energy. The radio between there three parameters will affect the formation of the spin texture. Then, the domain energy of the system can be explained as below:

$$\sigma_{DW} = 4\sqrt{AK_{eff}} - \pi|D| \quad (3)$$

With the temperature dependent parameters, the temperature dependent domain energy can be determined. From the simulation results, when the system temperature increases, the energy of the magnetic domains in the system will decrease. The energy barrier between the ferromagnetic state and domain state will reduce to a smaller value. Thus, it will be easier to generate magnetic domains in the system which is also demonstrated by the experiment measurement in Fig. 3. Due to the different domain energy distribution in the system, the temperature gradient generated by the sample holder can be used to modulate the domain nucleation area.

5. Conclusion

In this work, the temperature-dependent magnetic properties in CoFeB/MgO thin film are studied by both VSM and Kerr hysteresis loops. The magnetic properties of thin film are strongly influenced by the thermal effect and the critical external field of domain nucleation can be controlled by the thermal effect. With the appropriate external magnetic field and assist of temperature gradient, the writing operation of spin texture at specific area can be realized. Our simulation results represent the correlation between domain energy distribution and temperature gradient. The experiment results also fit well with the atomistic simulation and explain the relationship between the thermal effect and spin texture nucleation in magnetic film. Our findings can provide guidelines for the development of the racetrack memories and other spin texture-based spintronics devices.

Acknowledgement

This work was supported by the "Chunhui" international cooperation Program (HZKY20220018),

National Key Research and Development Program of China (2022YFB4400200), National Natural Science Foundation of China (T2394474, T2394470, 12304136, 12241403), Guangdong Basic and Applied Basic Research Foundation (Grant No. 2022A1515110863, 2023A1515010837), and Project for Maiden Voyage of Guangzhou Basic and Applied Basic Research Scheme (Grant No. 2024A04J4186). Xiangyu Zheng, Kangning Xu and Wenjia Li contributed equally to this work.

Reference

[1] I. E. Dzialoshinskii, "Thermodynamic theory of weak ferromagnetism in antiferromagnetic substances," *Soviet Physics Jetp-Ussr,* vol. 5.6, 1957.

[2] T. Moriya, "Anisotropic Superexchange Interaction and Weak Ferromagnetism," *Physical Review,* vol. 120, no. 1, pp. 91-98, 1960, doi: 10.1103/PhysRev.120.91.

[3] S. Kim *et al.*, "Correlation of the Dzyaloshinskii-Moriya interaction with Heisenberg exchange and orbital asphericity," *Nat Commun,* vol. 9, no. 1, p. 1648, Apr 25 2018, doi: 10.1038/s41467-018-04017-x.

[4] S. Muhlbauer *et al.*, "Skyrmion lattice in a chiral magnet," *Science,* vol. 323, no. 5916, pp. 915-9, Feb 13 2009, doi: 10.1126/science.1166767.

[5] X. Z. Yu *et al.*, "Real-space observation of a two-dimensional skyrmion crystal," *Nature,* vol. 465, no. 7300, pp. 901-4, Jun 17 2010, doi: 10.1038/nature09124.

[6] H. Yin *et al.*, "Defect-correlated skyrmions and controllable generation in perpendicularly magnetized CoFeB ultrathin films," *Applied Physics Letters,* vol. 119, no. 6, 2021, doi: 10.1063/5.0057763.

[7] S. Emori, U. Bauer, S. M. Ahn, E. Martinez, and G. S. Beach, "Current-driven dynamics of chiral ferromagnetic domain walls," *Nat Mater,* vol. 12, no. 7, pp. 611-6, Jul 2013, doi: 10.1038/nmat3675.

[8] A. Fert, V. Cros, and J. Sampaio, "Skyrmions on the track," *Nat Nanotechnol,* vol. 8, no. 3, pp. 152-6, Mar 2013, doi: 10.1038/nnano.2013.29.

[9] C. Ye *et al.*, "Generation and manipulation of skyrmions and other topological spin structures with rare metals," *Rare Metals,* vol. 41, no. 7, pp. 2200-2216, 2022, doi: 10.1007/s12598-021-01908-9.

[10] Y. Shu *et al.*, "Realization of the skyrmionic logic gates and diodes in the same racetrack with enhanced and modified edges," *Applied Physics Letters,* vol. 121, no. 4, 2022, doi: 10.1063/5.0097152.

[11] G. Yu *et al.*, "Room-Temperature Creation and Spin-Orbit Torque Manipulation of Skyrmions in Thin Films with Engineered Asymmetry," *Nano Lett,* vol. 16, no. 3, pp. 1981-8, Mar 9 2016, doi: 10.1021/acs.nanolett.5b05257.

[12] Q. Yang *et al.*, "Voltage Control of Skyrmion Bubbles for Topological Flexible Spintronic Devices," *Advanced Electronic Materials,* vol. 6, no. 8, 2020, doi: 10.1002/aelm.202000246.

[13] L. You *et al.*, "Switching of perpendicularly polarized nanomagnets with spin orbit torque without an external magnetic field by engineering a tilted anisotropy," *Proc Natl Acad Sci U S A,* vol. 112, no. 33, pp. 10310-5, Aug 18 2015, doi: 10.1073/pnas.1507474112.

[14] J. Liu, G. Y. Tian, B. Gao, K. Zeng, Y. Zheng, and J. Chen, "Micro-macro characteristics between domain wall motion and magnetic Barkhausen noise under tensile stress," *Journal of Magnetism and Magnetic Materials,* vol. 493, 2020, doi: 10.1016/j.jmmm.2019.165719.

[15] J. Wells *et al.*, "Combined anomalous Nernst effect and thermography studies of ultrathin CoFeB/Pt nanowires," *AIP Advances,* vol. 7, no. 5, 2017, doi: 10.1063/1.4973196.

[16] T. Böhnert, V. Vega, A.-K. Michel, V. M. Prida, and K. Nielsch, "Magneto-thermopower and magnetoresistance of single Co-Ni alloy nanowires," *Applied Physics Letters,* vol. 103, no. 9, 2013, doi: 10.1063/1.4819949.

[17] U. Martens *et al.*, "Anomalous Nernst effect and three-dimensional temperature gradients in magnetic tunnel junctions," *Communications Physics,* vol. 1, no. 1, 2018, doi: 10.1038/s42005-018-0063-y.

[18] C. M. Jaworski, J. Yang, S. Mack, D. D. Awschalom, J. P. Heremans, and R. C. Myers, "Observation of the spin-Seebeck effect in a ferromagnetic semiconductor," *Nat Mater,* vol. 9, no. 11, pp. 898-903, Nov 2010, doi: 10.1038/nmat2860.

[19] Z. Wang *et al.*, "Thermal generation, manipulation and thermoelectric detection of skyrmions," *Nature Electronics,* vol. 3, no. 11, pp. 672-679, 2020, doi: 10.1038/s41928-020-00489-2.

[20] S. Ikeda *et al.*, "A perpendicular-anisotropy CoFeB-MgO magnetic tunnel junction," *Nat Mater,* vol. 9, no. 9, pp. 721-4, Sep 2010, doi: 10.1038/nmat2804.

[21] M. Endo, S. Kanai, S. Ikeda, F. Matsukura, and H. Ohno, "Electric-field effects on thickness dependent magnetic anisotropy of sputtered MgO/Co40Fe40B20/Ta structures," *Applied Physics Letters,* vol. 96, no. 21, 2010, doi: 10.1063/1.3429592.

[22] *Microstat-family-of-cryostats*. Oxford Instruments.

[23] S. Li *et al.*, "Rich topological spin textures in single-phase and core-shell magnetic nanodisks," *Physical Review B,* vol. 107, no. 1, 2023, doi: 10.1103/PhysRevB.107.014414.

[24] "VAMPIRE software package, version 3, available from http://vampire.york.ac.uk/." (accessed.

[25] R. F. Evans, W. J. Fan, P. Chureemart, T. A. Ostler, M. O. Ellis, and R. W. Chantrell, "Atomistic spin model simulations of magnetic nanomaterials," *J Phys Condens Matter,* vol. 26, no. 10, p. 103202, Mar 12 2014, doi: 10.1088/0953-8984/26/10/103202.

[26] R. Tomasello *et al.*, "Origin of temperature and field dependence of magnetic skyrmion size in ultrathin nanodots," *Physical Review B,* vol. 97, no. 6, 2018, doi: 10.1103/PhysRevB.97.060402.